Anisotropic Mechanical Behaviour of Nickel Base Single Crystal Superalloy CMSX-4 for Prediction of Grain Recrystallization during Homogenization Heat-treatment Following Solidification

Emile Hazemann, Yancheng Zhang, Karim Inal, Charles-André Gandin, Ming Long, Ngadia Tahane Niane, Vincent Maguin, Mylène Leduc, Virginie Jaquet, Michel Bellet

Anisotropic Mechanical Behaviour of Nickel Base Single Crystal Superalloy CMSX-4 for Prediction of Grain Recrystallization during Homogenization Heat-treatment Following Solidification

E Hazemann[1, 2], Y Zhang[2], K Inal[2], Ch A Gandin[2], M Long[1], N T Niane[3], V Maguin[1], M Leduc[1], V Jaquet[1] and M Bellet[2]

[1] Safran Advanced Turbine Airfoils, 171 Boulevard Valmy, 92700 Colombes, France
[2] Mines Paris, PSL Research University, Centre de Mise en Forme des Matériaux, UMR CNRS 7635, Sophia Antipolis 06904, France
[3] Safran Aircraft Engines, 171 Boulevard Valmy, 92700 Colombes, France

Abstract. In the present work, the methodology to identify parameters of an elastic viscoplastic behaviour law is presented. Orthotropic elasticity and Hill48 plastic anisotropy for as-cast CMSX-4 are considered. In order to obtain the corresponding parameters by inverse analysis, an experimental database is built by tensile/relaxation tests at constant temperatures between 800°C and 1200°C on specimens oriented along <001>, <110> and <111> directions at different strain rates. Tests are performed with a resistive heating machine, using infrared thermography and digital image correlation. The obtained mechanical behaviour is very dependent on the orientations of the specimens at all tested temperatures, and especially for the deformation mechanisms. Recrystallization behaviour is also very relevant to the specimens' orientation.

1. Introduction

In jet engines, high pressure turbine blades undergo the most severe operating conditions. To face both extreme temperature and stress, single crystal nickel base superalloys are extensively used as they show higher resistance to creep and thermal fatigue compared to conventional microstructures. Their composition is characterized by the absence of grain boundaries strengthening elements. As a result, the presence of unexpected grain boundaries, caused by defects such as recrystallized grains (RGs), is seriously detrimental to the mechanical performances of the final part. Recrystallization is related to the accumulated plastic strain introduced during solidification and cooling of the molten alloy when casting a part. Being a thermally activated phenomenon, recrystallization may occur during the homogenization heat treatment that follows solidification.

In order to predict accurately RGs occurrence in a turbine blade, a representative description – through finite element calculation – of stresses and strains formed during the casting process is required. Therefore, an anisotropic elastic-viscoplastic behaviour law of the single crystal nickel-based superalloy in the as-cast state is necessary.

Different works have studied the conditions of recrystallization occurrence with different thermomechanical process such as indentation, compression or traction at different temperatures [Zam2007, Cox2003, Pan2013, Li2015]. The effects of deformation temperature, level of plastic strain, annealing temperature have been established in these studies. However, stresses were studied at a constant temperature, which is not representative of the mechanical load undergone by a turbine blade

during solidification. These studies are focused on the conditions of recrystallization occurrence, not aiming at the understanding of the elementary occurrence mechanism.
The present paper gives a methodology to identify parameters of a behaviour law for as-cast CMSX-4 with elastic and plastic anisotropy considerations. Thermomechanical tensile tests with constant cooling rate and loading ramp are presented for three different orientations of specimens to reproduce solidification and cooling paths of CMSX-4 in a turbine blade. These specimens are subjected to subsequent standard homogenization heat treatment to reveal recrystallization occurrence.

2. Materials and Methods

2.1. Tensile samples oriented along <001>, <110> and <111> directions

Second generation nickel-based superalloy CMSX-4 in the as-cast state was used for this investigation. Its composition is given in table 1. Several plates of 50 x10 x145 mm^3 and 80 x10 x 165 mm^3 were cast in Bridgman type furnace using respectively grain selector and single crystal seeds. Casting process followed industrial procedure at Safran Advanced Turbine Airfoils.
Tensile specimens were machined by Electro Discharge Machining (EDM) within plates of 50 x10 x145 mm^3 for samples with tensile direction aligned with <100> crystallographic orientation. Samples with tensile direction aligned with <110> or <111> crystallographic orientation were obtained within plates of 80 x10 x 165 mm^3 by EDM. Samples are cut off by 1 mm from each surface to avoid surface defects. The exact orientation of tensile specimens was measured by X-Ray Diffraction (XRD). Only specimens with less than 10° of misorientation were used in this study. Standard electrochemical etching technique was performed in Safran Advanced Turbine Airfoils to ensure that neither stray grains, multi-crystals nor freckles were present in gauge part of tensile specimen. Additional etching using 5 % HF, 27.6 % HNO_3, 67.4 % H_2O for 60 minutes removed residual surface affected by EDM. As-cast microstructure cartographies of one specimen oriented along the <001> direction were obtained by Scanning Electron Microscopy (SEM) with Zeiss Supra 40 apparatus [Zei2022]. Local composition was measured on two specimens oriented along <001> by Energy Dispersive Spectroscopy (EDS) at different heights to account for macrosegregation with Brücker system and Maya3 Tescan apparatus [Bru2022, Pol2022]. For SEM imaging and EDS analyses, samples were cut on a XY plane (figure 1) and mechanically polished to a final step of colloidal silica. A high voltage of 20 kV was used for the imaging.

Table 1. Nominal composition of CMSX-4.

Element	Al	Co	Cr	Hf	Mo	Ni	Re	Ta	Ti	W
wt%	5.6	9.7	6.4	0.1	0.6	Balance	3.0	6.5	1.0	6.4

2.2. Tensile tests at high temperature for behaviour law identification

Tests are conducted in tensile machine DEDIMET developed at CEMEF [Pig2018, Gao2022]. A schematic view of the sample in the machine is presented in figure 1. The sample is heated by Joule effect. All the tests are carried out under primary vacuum conditions to limit oxide formation on sample surface. Tests are performed at a constant nominal temperature between 1000 and 1200 °C. Setpoint temperature is monitored by a type K thermocouple welded at mid hight of the gauge length. A bichromatic pyrometer and an Infra-Red (IR) camera measure maximum temperature and temperature field, respectively, within the gauge length. The upper jaw is fixed, setpoint velocity is imposed on the lower jaw. The machine is monitored by a Labview code [Lab2022]. During heating and cooling, a zero-set point load is fixed to prevent stresses caused by thermal dilatation/contraction. With Joule effect heating, strain is localized due to high vertical temperature gradient. Strain and displacement are tracked locally within gauge length with Digital Image Correlation (DIC). Temperature resistant speckles made of Aremco Pyro-Paint 634-ALP are applied on samples surface [Are2022]. VIC-Snap is used for images acquisition [Sut2009]. Two cameras Point Grey Grasshopper2 are used for the tests in the same vertical axis with an angle inferior to 30° between them [Fli2022]. They are combined with Schneider-kreuznach xenoplan 2.0/280901 15218330 optics [Sch2022]. Acquisition frequency varies between 5 and 10 Hz.

VIC-3D is used to analyse images to obtain displacement and deformation of the speckles in the gauge length with respect to a reference image [Sut2009].
For each sample, 3 cycles of tensile/relaxation phases are performed with respectively 0.01, 0.003 and 0.008 mm. s^{-1} set point velocities for the three tensile cycles. Duration of each tensile phase depends on set point temperature and is adapted to introduce up to 20% of deformation within the gauge length at the end of the test. Durations were calculated using preliminary tensile tests with one tensile/relaxation phase. Heating rate and cooling rate were 6 °C. s^{-1} and -7.5 °C. s^{-1}, respectively. A temperature stabilisation step of 100 s precedes the first tensile/relaxation cycle.

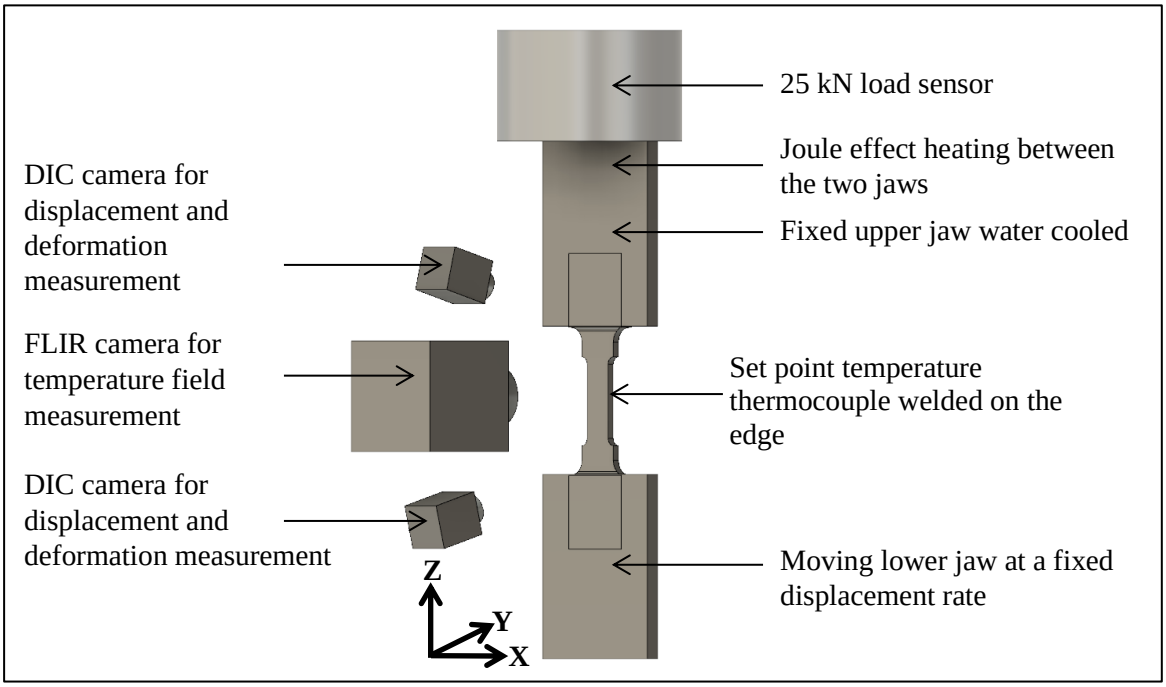

Figure 1. Schematic view of tensile testing machine DEDIMET.

2.3. Tensile tests at high temperature, constant cooling rate and constant load rate for recrystallization criterion identification

Additional thermomechanical tests with constant cooling rate and load ramp are performed in DEDIMET to study recrystallization occurrence. This type of test is presented in figure 2. The tests parameters are gathered in table 2. Three different tests with various final loading F_{end} were carried out on specimens oriented along the <100>, <110> and <111> directions. Set point temperature was monitored with a bichromatic pyrometer.

Table 2. Testing parameters of non-isothermal tests.

T_{init} (°C)	$\dot{T}_{init}$ (°C.s^{-1})	$\dot{T}_{tensile}$ (°C.min^{-1})	$\dot{T}_{end}$ (°C.s^{-1})	F_{init} (N)	F_{end} (N)	$t_{tensile}$ (s)	$t_{tinit.}$ (s)	$t_{stab.}$ (s)
1200	6	-10.6	-7.5	1000	7000 9600	2300	500	60

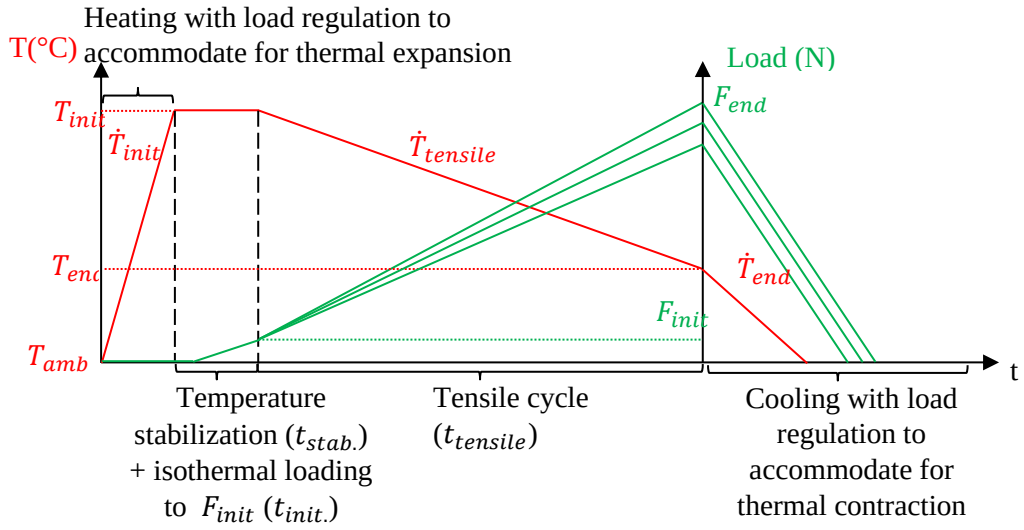

Figure 2. Schematic representation of non-isothermal tests.

2.4. Homogenization heat treatment and subsequent etching to highlight recrystallization occurrence
Specimens used for non-isothermal tests were subjected to the standard homogenization heat treatment in a primary vacuum heat treatment furnace Carbolite STF16-180 [Dat2022]. Specimens were attacked for 2 hours with Kalling etchant to highlight RGs when recrystallization occurred [Zam2007].

3. Mathematical model

3.1. Behaviour law
Only main equations are presented in this work. More details can be found elsewhere [Gao2022]. The mathematical model is implemented in a library developed at CEMEF (Cimlib).
For small strains, one can assume an additive decomposition for the strain rate:

$$\dot{\boldsymbol{\varepsilon}} = \dot{\boldsymbol{\varepsilon}}^{\boldsymbol{el}} + \dot{\boldsymbol{\varepsilon}}^{\boldsymbol{vp}} + \dot{\boldsymbol{\varepsilon}}^{\boldsymbol{th}} \quad (1)$$

With $\dot{\boldsymbol{\varepsilon}}^{\boldsymbol{el}}$, $\dot{\boldsymbol{\varepsilon}}^{\boldsymbol{vp}}$ and $\dot{\boldsymbol{\varepsilon}}^{\boldsymbol{th}}$ respectively the elastic, viscoplastic and thermal contributions to the strain rate tensor. The elastic strain rate is adapted for orthotropic properties. To consider anisotropic plasticity, Hill48 criterion adapted for orthotropic material is chosen [Hill1948].
The developed expression for the behaviour law is as follows:

$$\bar{\sigma} = \left(\sigma_{Y0,T_{ref}} + Q_{T_{ref}} * \left(1 - \exp(-b\bar{\varepsilon})\right)\right) * \exp\left[\frac{Q_1}{R}\left(\frac{1}{T} - \frac{1}{T_{ref}}\right)\right] + k_{T_{ref}}\dot{\bar{\varepsilon}}^{m} * \exp\left[\frac{Q_2}{R}\left(\frac{1}{T} - \frac{1}{T_{ref}}\right)\right] \quad (2)$$

With Q_1 and Q_2 activation energies and T_{ref} the reference temperature.

3.2. Boundary conditions of the model
Only the gauge length is considered in the model. Temperature profile is directly imposed and velocity along tensile direction Z is considered as the boundary conditions during the simulation. They both are adapted from experimental measurements. More detailed methodology is presented in [Gao2022].

3.3. Identification strategy
An inverse analysis software developed at CEMEF is used to identify the different parameters of the behaviour law. Optimization strategy is similar to the one presented in [Gao2022]. Cost function expression is as follows:

$$F_c = \sqrt{\frac{\sum_i \left(F_{i,j}{}^{exp} - F_{i,j}{}^{sim}\right)^2}{\sum_i \left(F_{i,j}{}^{exp}\right)^2}} \quad (3)$$

Considering the high total number of parameters used in the model, elastic properties were chosen as inputs, which are tabulated with temperature. Values are adapted from [Her1996].
First step of identification strategy was to identify all the parameters for the orientation <001>.
After identifying all the parameters for <001> orientation, grouped optimizations are performed for one temperature and three different orientations. All the parameters are identified in this step, including the plastic anisotropy factor.

4. Results and Discussion

4.1. Model development

The results of grouped optimization for specimens oriented along <001> direction at 1021°C, 1116°C and 1201°C are presented in figure 3. The 3 tensile/relaxation cycles are indicated by the vertical dashed lines for the specimen deformed at 1021°C. One can see very good agreement between simulated and experimental loads is obtained. Even though elastic properties are given as inputs of the model, simulated elastic part agrees well with experimental data. One can conclude that the model can predict accurately the behaviour of CMSX-4 between 1021°C and 1201°C for the orientation <001>. Grouped optimization for <001> orientation and more temperatures are ongoing.
Model inputs for anisotropy consideration are Euler angles. Results obtained for elastic part between <001> and <111> directions at 1000°C have been compared with analytical calculations to validate the model. Grouped optimizations for one temperature and three orientations are ongoing to identify plastic anisotropy factor.

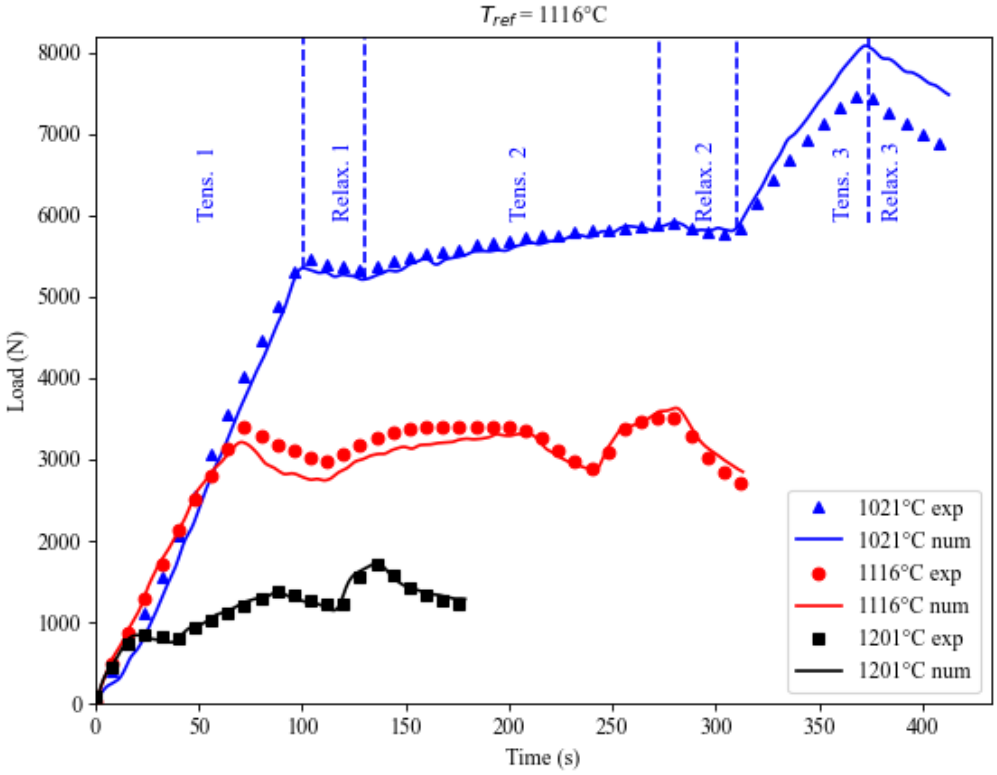

Figure 3. Grouped optimization for <001> oriented specimens at 1021, 1116 and 1201 °C.

4.2. Recrystallization occurrence

Optical micrographs of specimens oriented along <111> direction after non-isothermal load ramps to 7000 N and 9600 N, homogenization heat treatment and attacked by Kalling etchant are presented in figures 4 and 5, respectively. No recrystallization is visible on gauge length for the specimen loaded up

to 7000 N, while numerous RGs are visible on almost all gauge length for specimen loaded up to 9600 N. Additionally, one can observe strong necking for the latter, indicating large plastic strain compared to the sample loaded to 7000 N. Interestingly, most of the recrystallized grain boundaries appear to follow the direction of the primary dendritic arms. Recrystallized grain size is quite large, indicating that only few orientations were favoured to grow.

The results for recrystallization occurrence of three different orientations and two different load ramps are gathered in table 3. The absence of recrystallization is indicated with a - mark. Recrystallization occurrence is evaluated qualitatively between + and +++ marks, with + the smallest recrystallized zone and +++ the largest. For ramp to 9600 N, one can conclude that specimen orientation has significant effect on recrystallization occurrence: recrystallized area is larger for specimen oriented along <111> direction than <100> direction, while no recrystallization is visible for specimen oriented along <110> direction. A recrystallization criterion can be identified in term of load ramp at constant cooling rate between 7000 and 9600 N for <111> oriented specimens. For <110> orientation, a load ramp up to a higher value than 9600 N is necessary. For <100> orientation, two more tests are required up to 5000 N and 7000 N to identify a recrystallization criterion.

Figure 4. <111> specimen after non-isothermal loading up to 7000 N, standard homogenization heat treatment and subsequent etching.

Figure 4. <111> specimen after non-isothermal loading up to 9600 N, standard homogenization heat treatment and subsequent etching.

Table 3. Recrystallization results for non-isothermal tests of three different orientations.

F_{end} (N)	7000	9600
<001>		++
<110>	-	-
<111>	-	+++

Following steps include the simulation of non-isothermal load ramps for the different orientations with the previously presented behaviour law to identify a recrystallization criterion among all simulated quantities. These simulations are ongoing to choose the quantity that fits the best recrystallization behaviour with orientation consideration.

5. Conclusions

A methodology to identify parameters of anisotropic elastic viscoplastic behaviour law for as-cast CMSX-4 has been presented. Results show that parameters identified for <100> orientation and temperature between 1021°C and 1201°C agrees well with experimental results. Developments to include more temperatures for parameters identification are ongoing. Plastic and elastic anisotropies are considered in the model, identification of plastic anisotropy factor for different temperatures is ongoing. Elastic anisotropy has been validated with analytic calculations.

Orientation appears to have a strong effect on recrystallization behaviour for specimens tested on non-isothermal load ramps with subsequent homogenization heat treatment. Ongoing works include direct simulation on thermomechanical paths to identify a recrystallization criterion. Additionally, several experimental tests are still required to identify a restrained window of recrystallization occurrence for <001> and <110> oriented specimens.

6. References

[Are2022] https://www.aremco.com/high-temp-refractory-coatings/
Last consulted: 2022/01/25

[Bru2022] https://www.bruker.com/en/products-and-solutions/elemental-analyzers/eds-wds-ebsd-SEM-Micro-XRF/software-esprit-family.html
Last consulted: 2022/01/25

[Cox2003] Cox, D C, Roebuck, B, Rae, C M F, & Reed, R C (2003). Recrystallisation of single crystal superalloy CMSX–4. *Materials Science and Technology*, **19**(4), 440–446. https://doi.org/10.1179/026708303225010731

[Dat2022] https://datasheets.globalspec.com/ds/3961/CARBOLITEGERO/C66B7056-7922-48C0-9461-60924048CDD1
Last consulted: 2022/01/25

[Fli2022] https://flir.app.boxcn.net/s/btwotjdov5nh89u0qewxyj5ro6hh2qyj/file/418659124558
Last consulted 2022/01/25

[Gao2022] Gao F, Macquaire B, Zhang Y, Bellet M (2022). A new localized inverse identification method for high temperature testing under resistive heating: Application to the elastic-viscoplastic behaviour of L-PBF processed In718. Strain. DOI: doi.org/10.1111/str.12409

[Hill1948] Hill, R (1948) A theory of the yielding and plastic flow of anisotropic metals. *Proc. Roy. Soc. London A*, **193**, pp. 281-297

[Her1996] Hermann, W, Sockel, HG, Han, J, Bertram, A (1996). Elastic properties and determination of elastic constants of nickel-based superalloys by a free-free beam technique. Superalloys 1996, *The minerals, Metals & Materials Society*.

[Lab2022] https://www.ni.com/fr-fr/shop/labview.html
Last consulted 2022/01/25

[Li2015] Li, Z, Xiong, J, Xu, Q, Li, J, & Liu, B (2015). Deformation and recrystallization of single crystal nickel-based superalloys during investment casting. *Journal of Materials Processing Technology*, **217**(March 2015), 1–12. https://doi.org/10.1016/j.jmatprotec.2014.10.019

[Pan2013] Panwisawas, C, Mathur, H, Gebelin, J, Putman, D, Rae, C M F, & Reed, R C (2013). Prediction of recrystallization in investment cast single-crystal superalloys. *Acta Materialia*, **61**(1), 51–66. https://doi.org/10.1016/j.actamat.2012.09.013

[Pig2018] Pignolet, A, Combeaud, C, Fournier, F, Fiorucci, G, Pradille, C, Zhang, Y, Pinto-Mora, A, Gao, F, Bellet, M (2018). Experimental approach for metals mechanical behaviour characterization at high temperature: development of a complex tensile test machine, ICEM18, *18th Int. Conf. on Experimental Mechanics*, Brussels, July 1-5, 2018, in Proceedings, an open access journal published by the Multidisciplinary Digital Publishing Institute, vol. 2 355-360

[Pol2022] https://www.polyu.edu.hk/umf/facility/mrc/110-field-emission-scanning-electron-microscope-tescan-maia3/
Last consulted: 2022/01/25

[Rou2020] Roux, E, Tillier, Y, Kraria, S, Bouchard, PO (2020). An efficient parallel global optimization strategy based on Krieging properties suitable for material parameters identification. *Archive of mechanical engineering 2020*.
DOI: 10.24425/ame.2020.131689

[Sch2022] https://www.google.com/url?sa=t&rct=j&q=&esrc=s&source=web&cd=&ved=2ahUKEwah8p2m-cz1AhXuzoUKHQNNDLMQFnoECAYQAQ&url=https%3A%2F%2Fcdn.alliedvision.coc%2Ffileadmin%2Fcontent%2Fdocuments%2Fproducts%2Faccessories%2Flenses%2FSchneider%2FData_sheet%2F1001972_Xenoplan_2.0-28.pdf&usg=AOvVaw3XUX0icxUNwzl1kUlsccBG
Last consulted 2022/01/25

[Sut2009] Sutton, M A, Orteu, J J, Schreier, H W (2009). Image Correlation for Shape, Motion and Deformation Measurements. Basic Concepts, Theory and Applications. DOI: 10.1007/978-0-387-78747-3

[Zam2007] Zambaldi, C, Roters, F, Raabe, D, & Glatzel, U (2007). Modelling and experiments on the indentation deformation and recrystallization of a single-crystal nickel-base superalloy., 454–455, 433–440. https://doi.org/10.1016/j.msea.2006.11.068

[Zei2022] https://wiki.smfi.unipr.it/dokuwiki/lib/exe/fetch.php?media=lmn:brochure.pdf
Last consulted: 2022/01/25

Acknowledgments
The authors are thankful to all the CEMEF staff that helped for preparation of specimens, microscopic observations and mechanical discussion: Cyrille Collin, Gilbert Fiorucci, Christophe Pradille, Salim Kraria, Guillaume Corvec, Arnaud Pignolet and Francis Fournier.